EARTHQUAKE ENGINEERING AND STRUCTURAL DYNAMICS, VOL. 26, 1073–1088 (1997)

VERIFICATION OF SEISMIC RESISTANCE OF CONFINED MASONRY BUILDINGS

MIHA TOMAŽEVIČ* AND IZTOK KLEMENC

Slovenian National Building and Civil Engineering Institute, Dimičeva 12, 1000 Ljubljana, Slovenia

SUMMARY

Two models of a typical confined masonry building, which conforms to the requirements of Eurocode 8 for simple buildings, have been tested on a shaking-table. Model test results indicate that prototypes of the tested type and size will be able to withstand, with moderate damage to the walls, strong earthquakes with peak ground acceleration $0{\cdot}8g$, and will not collapse when subjected to repeated shaking with PGA more than $1{\cdot}3g$. Taking into consideration the observed predominant first vibration mode shape and shear-beam-type shape of vibration, a rational method for seismic resistance verification of confined masonry structures has been proposed, modelling the confined masonry shear walls as frames. Good correlation between experimental and calculated envelopes has been obtained, indicating the validity of the proposed method. The measured response of the models has also been used to analyse the value of behaviour factor q proposed by EC 8 for confined masonry structures. © 1997 John Wiley & Sons, Ltd.

Earthquake Engng. Struct. Dyn., **26**, 1073–1088 (1997)

No. of Figures: 11. No. of Tables: 6. No. of References: 12.

KEY WORDS: confined masonry; seismic behaviour; resistance; mathematical model; behaviour factor

INTRODUCTION

The basic feature of confined masonry construction systems are vertical reinforced-concrete or reinforced-masonry elements, tie-columns, which confine the masonry walls along their vertical edges. Tie-columns are usually placed at all corners and wall intersections, as well as along the vertical edges of door and window openings, and their reinforcement should be well connected with the reinforcement of horizontal bonding elements. Traditionally, r.c. confining elements do not represent the load-bearing part of the structure. In most cases, the amount of their reinforcement is determined by experience and depends on the height and size of the building.

Although confined masonry is one of the most widely used masonry construction systems in Europe, Asia, and Latin America, limited experimental research into the seismic behaviour of confined masonry buildings has been carried out so far to provide data for the development of rational methods for their seismic resistance verification. Consequently, according to the requirements of recent Eurocodes 6 and 8,[1,2] no contribution of vertical confinement to vertical and lateral resistance of the structure should be taken into account in the calculation, although the tie-columns improve the ductility and lateral resistance of structural walls.[3–6] Tie-columns also improve the seismic behaviour of buildings. As shown by Bolong *et al.*,[7] who investigated the behaviour of scaled models of a five-storey house, a limited number of tie-columns placed at the corners of building already improved the resistance with respect to similar plain masonry house.

* Correspondence to: Miha Tomaževič, ZAG Ljubljana, Slovenian National Building and Civil Engineering Institute, Dimičeva 12, 1000 Ljubljana, Slovenia

Contract grant sponsor: Ministry of Science and Technology of the Republic of Slovenia; Contract grant number: J2-5208-1502

CCC 0098–8847/97/101073–16$17·50

Received 26 November 1996
Revised 11 March 1997

Bolong *et al.*[7] concluded that increased number of vertical tie-columns would further increase the building's seismic resistance.

To obtain additional data regarding the seismic behaviour, two models of a typical three-storey confined masonry building have been recently tested on the shaking-table at Slovenian National Building and Civil Engineering Institute (ZAG) in Ljubljana, Slovenia. The experiments have been aimed at investigating the mechanism of seismic behaviour and obtaining data needed for the development of a rational method for seismic resistance verification.

DESCRIPTION OF EXPERIMENTS

The structural system of the prototype consists of perimetral walls, pierced with window and/or door openings on all four sides, and two internal walls, which separate the plan of the building into four units. Whereas the building is symmetrical in the shorter direction, a slight asymmetry in the longer direction is a result of non-symmetric position of openings along the walls, as well as non-symmetric position of internal wall in that direction. Floors are monolithic reinforced-concrete, cast *in situ* slabs, supported by structural walls in both orthogonal directions. Although the dimensions of models, built at 1:5 scale, have been accommodated to the dimensions of the steel platform of the shaking-table at ZAG, the dimensions and structural characteristics of the corresponding actual prototype building are still within the limits of usual design practice (wall/floor area ratio being 5·0 per cent in longitudinal and 5·6 per cent in transverse direction

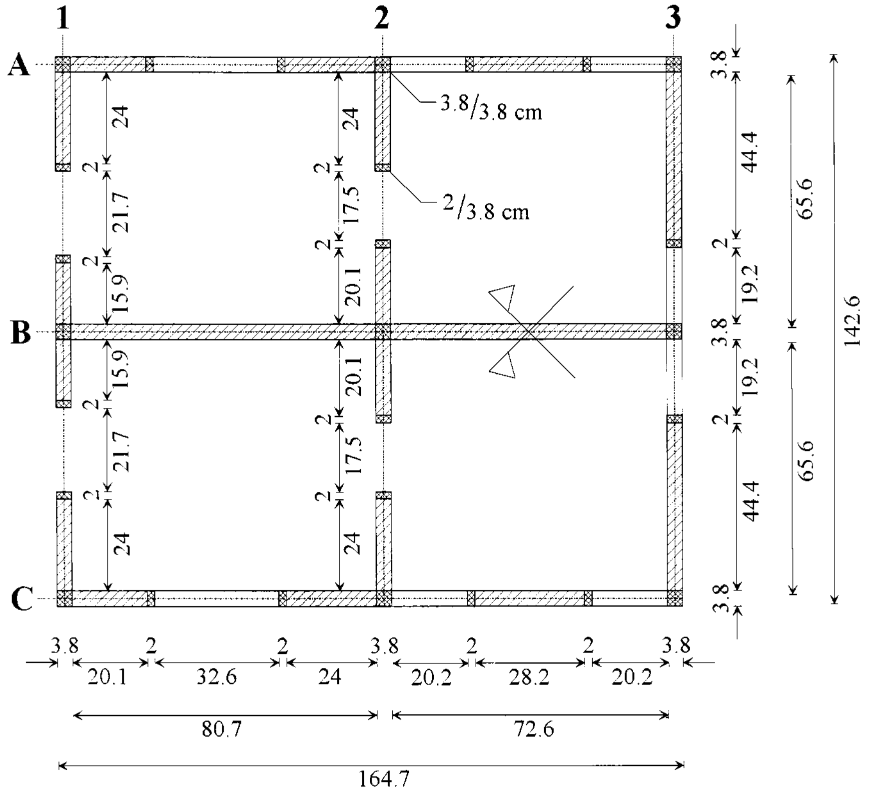

Figure 1. Disposition of tie-columns and dimensions of models in plan (in cm)

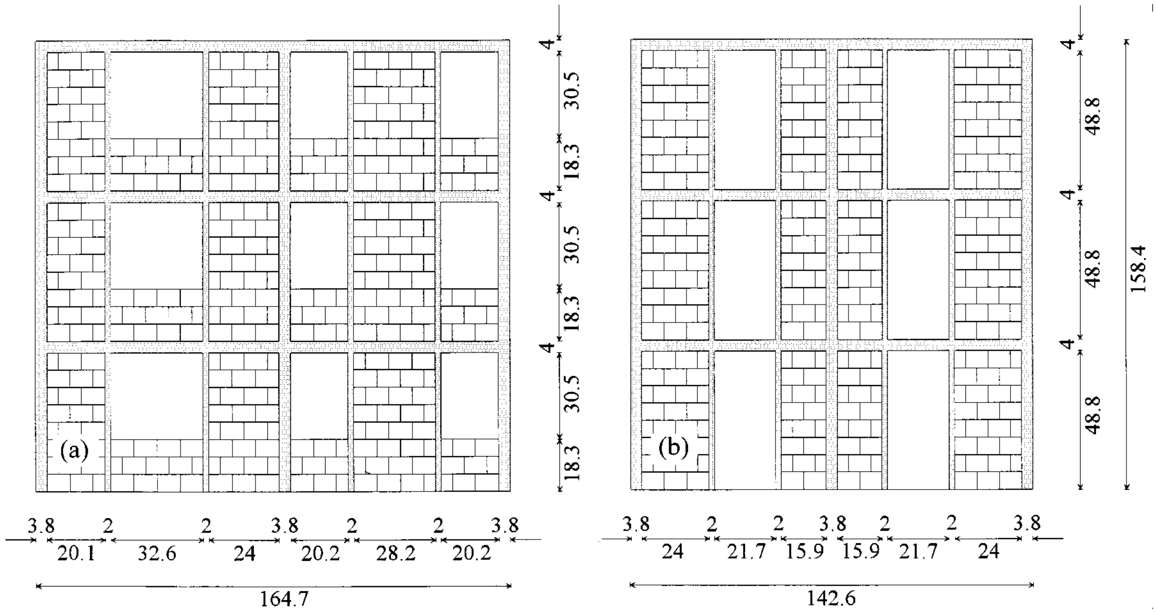

Figure 2. Disposition of tie-columns and dimensions of models in elevation. Shear walls A and C (a) and (b) shear wall 1 (in cm)

Table I. Mechanical properties of prototype and model materials

	Prototype	Model	Prot./Model
Compressive strength of masonry	5·0 MPa	1·27 MPa	3·9
Tensile strength of masonry	0·35 MPa	0·12 MPa	2·9
Modulus of elasticity of masonry	3500 MPa	942 MPa	3·7
Shear modulus of masonry	500 MPa	185 MPa	2·7
Compressive strength of concrete	25·0 MPa	10·8 MPa	2·3
Yield stress of reinforcing steel	240·0 MPa	not modeled	—

of the building). The structural layout of the modified prototype building in plan conforms to the requirements of EC 8 for 'simple buildings'. For such buildings, an explicit verification of the seismic resistance is not mandatory. The dimensions of the models in plan and elevation are shown in Figures 1 and 2, respectively.

In the design of the models and model materials, the basic requirements of reproducing the dynamic behaviour and failure mechanism, i.e. the similarity in the distribution of masses and stiffnesses along the height of the prototype and the model, as well as similarity in the ratio between the working stresses in the walls and strength of masonry materials, have been followed. Consequently, model masonry materials that had the strength reduced close to the geometrical scale, but with the same strain characteristics, specific mass and damping, as prototype materials, have been prepared. Mechanical properties of prototype and model materials are given in Table I. The resulting modelling factors, however, which should be used when referring the model test results to prototype, are presented in Table II.

Commercially available fully annealed wire has been used to reinforce the tie-columns. Four bars, 3·2 mm diameter, have been used at corners and wall intersections, and 2 bars have been used at the vertical borders of door and window openings. In order to model the missing live load, lead bricks (160 kg at each floor level)

Table II. Modeling scale factors

Physical quantity	Modeling factor		
	Relationship	True model	This study
Length (L)	$S_L = L_P/L_M$	5	5
Strength (f)	$S_f = f_P/f_M = S_L$	5	2·92
Strain (ε)	$S_\varepsilon = \varepsilon_P/\varepsilon_M$	1	1
Sp. mass (γ)	$S_\gamma = \gamma_P/\gamma_M$	1	1
Displacement (d)	$S_d = S_L$	5	5
Force (F)	$S_F = S_L^2 S_f$	125	72·9
Time (t)	$S_L(S_\varepsilon S_\gamma/S_f)^{0.5}$	2·24	2·93
Frequency (ω)	$S_\omega = 1/S_t$	0·45	0·34
Velocity (v)	$S_v = (S_\varepsilon S_f/S_\gamma)^{0.5}$	2·24	1·71
Acceleration (a)	$S_a = S_f/(S_L S_\gamma)$	1	0·58

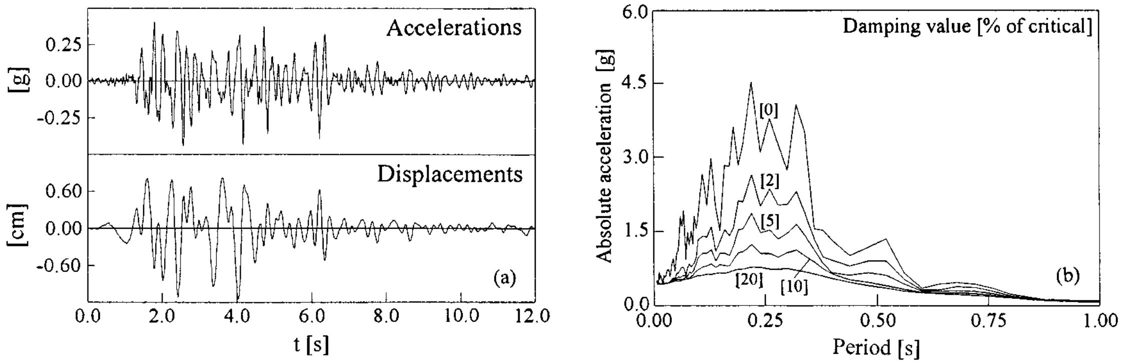

Figure 3. Modelled earthquake accelerogram (a) and (b) absolute acceleration response spectrum

were fixed to the floors, so that the resulting masses concentrated at first, second, and third floor level of the models amounted to 501, 501, and 377 kg, respectively.

The first 24 s of the ground acceleration record of Montenegro earthquake of 15 April 1979, N–S component recorded at Petrovac, with peak ground acceleration $0{\cdot}43g$[8] have been used for simulation of earthquake ground motion. Original record has been compressed in time by 2·24-times to take into account the chosen modelling scale and conditions of complete model similarity (Figure 3). However, displacement time history, obtained by integration of the modelled ground acceleration record, has been used to drive the shaking table.

Both models have been tested by subjecting them to the same sequence of seismic excitation, with gradually increased intensity of motion in each successive test run up until the final collapse of the models. Whereas model M1 has been tested longitudinally, model M2 was subjected to excitation along its transverse axis. In this way, possible torsional effects in the case of non-symmetric confined masonry structures could have been studied. The basic parameters of the shaking-table motion in each successive test run, such as maximum displacement and acceleration, as well as Arias intensity[9] and input energy per unit of mass, are given in Table III. Test runs are designated according to programmed input intensity of the shaking-table motion: R100 (100 per cent) corresponds to the modelled ground acceleration record. Typical instrumentation of the models is shown in Figure 4.

Table III. Characteristic parameters of shaking-table motion recorded during shaking-table tests

Model	Test run	Maximum displacement (mm)	Maximum acceleration (m/s^2)	Input energy (m^2/s^2)	Arias intensity (m/s)
M1	R5	0·87	1·12	0·002	0·26
	R25	3·38	4·05	0·066	6·65
	R50	6·35	9·27	0·236	25·02
	R75*	9·21	9·65	0·471	47·05
	R100†	12·45	14·23	0·777	78·46
	R150	18·53	17·08	1·879	190·34
	R200‡	24·29	28·31	2·536	238·64
M2	R5	1·00	1·02	0·002	0·19
	R25	3·17	3·93	0·071	7·43
	R50*	6·63	7·02	0·236	23·54
	R75	10·01	11·75	0·507	55·11
	R100†	12·74	13·85	0·961	113·81
	R150	18·92	17·56	1·688	179·28
	R200	24·27	23·42	2·385	234·01
	R200/1‡	23·72	20·84	2·436	237·62

Note: *Elastic limit, †maximum resistance, ‡ultimate state

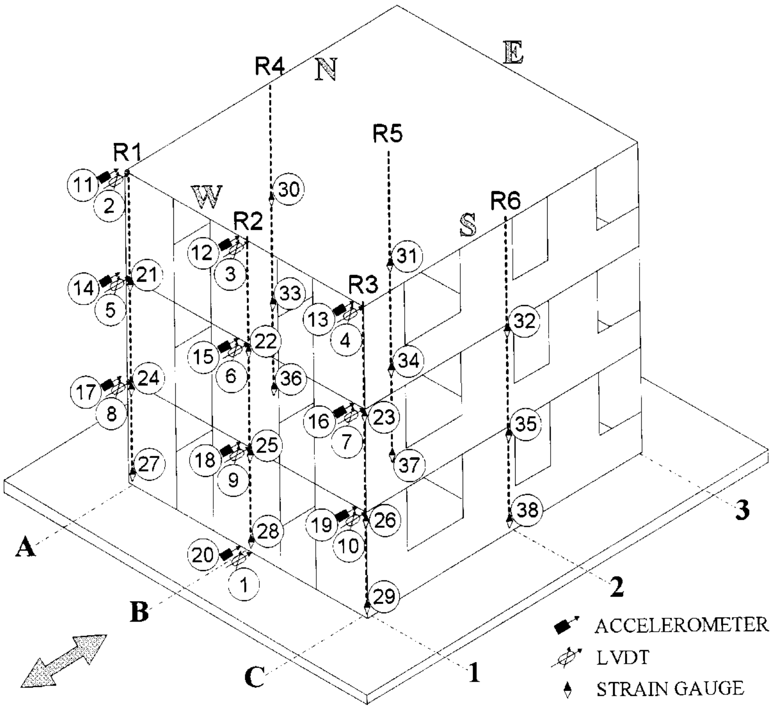

Figure 4. Instrumentation of model M1

EXPERIMENTAL RESULTS

Damage propagation and failure mechanism

The behaviour of both models was similar, although different position of models M1 and M2 on the platform and resulting different resistance, stiffness, and non-symmetry, caused slightly different damage propagation in the two cases. Diagonally oriented cracks in the middle part of perimetral walls in the direction of motion, have developed in the initial phases of testing. During the test runs to follow, the existing cracks propagated and new diagonal cracks formed, oriented in the other diagonal direction. Horizontal cracks, passing through mortar joints, have been observed in the parapets.

Model M1 has been seriously damaged during test run R150 (see Table III for the parameters of shaking table motion). In all storeys and in all walls standing in the direction of seismic excitation, a system of cracks developed, oriented in both diagonal directions. All parapets have been also damaged: in some of them, horizontal, in most of them, however, diagonally oriented cracks formed. Although most of the cracks passed through mortar joints, the initiation of crushing of masonry units has been also observed in the middle, most stressed parts of the walls, located in the first storey. After test run R150, cracks in the central wall in the direction of seismic motion have been also observed. Whereas horizontal cracks prevailed in that wall in the first, diagonal cracks occurred in the second storey. Although severe stiffness degradation of model M1 has been observed as a result of heavy damage to the walls, and, consequently, large displacement amplitudes of vibration have been measured, no damage has been observed to the walls, orthogonal to seismic excitation. Also, no damage has been observed to confining elements—tie-column and floor slabs.

Heavy structural damage occurred during test run R200. In the middle sections of the walls, located in the first floor, masonry units crushed, the walls separated from the confining elements, and disintegrated. Parts of the central wall failed in shear, in some parts, however, sliding shear failure was the reason of collapse. During test run R200 the amplitudes of vibration immensely increased, so that the walls orthogonal to seismic excitation broke. Horizontal cracks at the connection of the walls to the foundation and first floor slab, as well as diagonal cracks in the corner parts of these walls developed. Severe damage to vertical tie-columns has been also observed. Crushing of concrete took place at the joints between vertical tie-columns and horizontal bond-beams. In some cases, rupture of vertical reinforcing steel in tie-columns has been also observed.

Model M2 was seriously damaged during test run R100. A system of cracks, oriented in both diagonal directions, developed in all walls in the direction of seismic motion. Although most of the cracks passed through mortar joints, crushing of masonry units has been observed in the most stressed parts of wall elements. Cracks in the joints between masonry units have been observed in the parapets. However, no damage has been observed to shear-walls, orthogonal to the direction of seismic excitation.

During test run R150, crushed masonry units started falling off the walls of the first and second storey. Significant damage to elements of the central shear-wall, and damage to transverse parts of the corner walls occurred. The beginning of crushing of micro-concrete at the joints between vertical and horizontal tying elements has been also observed. The extent of damage to model M2 during test run R200 significantly changed the dynamic characteristics of the model. As was the case of model M1, practically all walls in the first storey (ground floor) disintegrated, so that only vertical confining elements supported the upper two storeys. Heavy damage occurred to r.c. tie-columns, whereas no damage to floor slabs has been observed. At the connection of vertical tie-columns to bond-beams or slabs, crushing of concrete and buckling of reinforcing steel took place. Because of large lateral displacements, damage to transverse walls in the first storey increased significantly.

To correlate the results of experiments with calculations and verify the proposed numerical model, three limit states have been defined in the behaviour of the models:

(a) Elastic limit, defined by the occurrence of the first major damage to the model's structural elements that caused noticeable decay of the first natural frequency of vibration,

Figure 5. Mechanism of collapse of model M2

(b) Maximum resistance, defined by the maximum base shear resisted, and
(c) Ultimate state, representing the characteristics of the models just before collapse (i.e., at the moment when the instruments have been removed from the models).

Typical damage to models at ultimate state is shown in Figure 5. The testing phases where the so-defined limit states have been observed, however, are indicated in Table III.

DYNAMIC RESPONSE

Typical recorded acceleration and displacement response time-histories at elastic limit (test run R50) and at ultimate state (test run R200) are shown in Figure 6. Since the analysis of the floor response indicated that the first vibration mode was predominant, the first vibration mode shape has been evaluated by taking into account the average values of three maximum displacement amplitudes at oscillations in positive and negative direction. The first vibration mode shapes at characteristic limit states are presented in Figure 7. Both models responded similarly, representing a shear-beam-type vibration system. In the last phases of testing, however, where the softening of the first storey due to disintegration of masonry walls changed the distribution of stiffnesses along the height, the models no longer vibrated as a shear beam.

The decay of the first natural frequency of vibration and changes in coefficient of equivalent viscous damping have been determined by analysing free vibration of the model, caused by hitting the model with impact hammer after each testing phase, as well as by analysing the seismic response. Half-power bandwidth method has been used to estimate the values of coefficient of equivalent viscous damping. The values of the first frequency of vibration and coefficient of equivalent viscous damping at characteristic limit states are given in Table IV.

As can be seen, frequency decay is in good correlation with the observed damage to structural walls. Significant differences between the values of natural frequencies obtained from free vibration records at small amplitudes of vibration at the end of each testing phase (impact hammer test), and those obtained by Fourier analysis of the models' response during the strong shaking, can be noticed. As regards the values of coefficient of equivalent viscous damping, the values obtained on the basis of logarithmic decrement of damping and

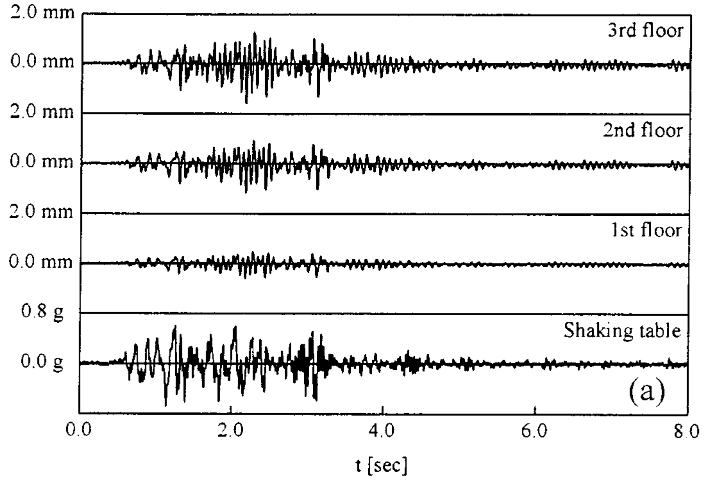

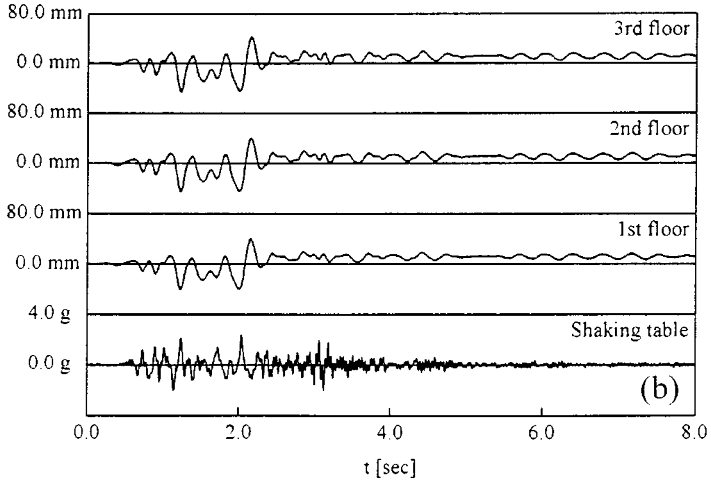

Figure 6. Typical measured displacement response time-histories in linear (a) and (b) in non-linear range of vibration

measured hysteretic behaviour seem more realistic than the values obtained by half-power bandwidth method.

Taking into consideration the predominant first vibration mode shape and shear-beam-type shape of vibration, and assuming that the observed first mode shape is stable during the shaking, and neglecting the damping, base shear and storey shear can be determined at each instant of time as a sum of inertia forces acting at floor levels:

$$\mathrm{BS} = \sum_{i}^{n} m_i a_i = \sum_{i}^{n} Q_i \tag{1}$$

where BS is the base shear, Q_i the ith storey shear, m_i the mass concentrated at ith storey level, a_i the acceleration of the ith mass and n the number of storeys.

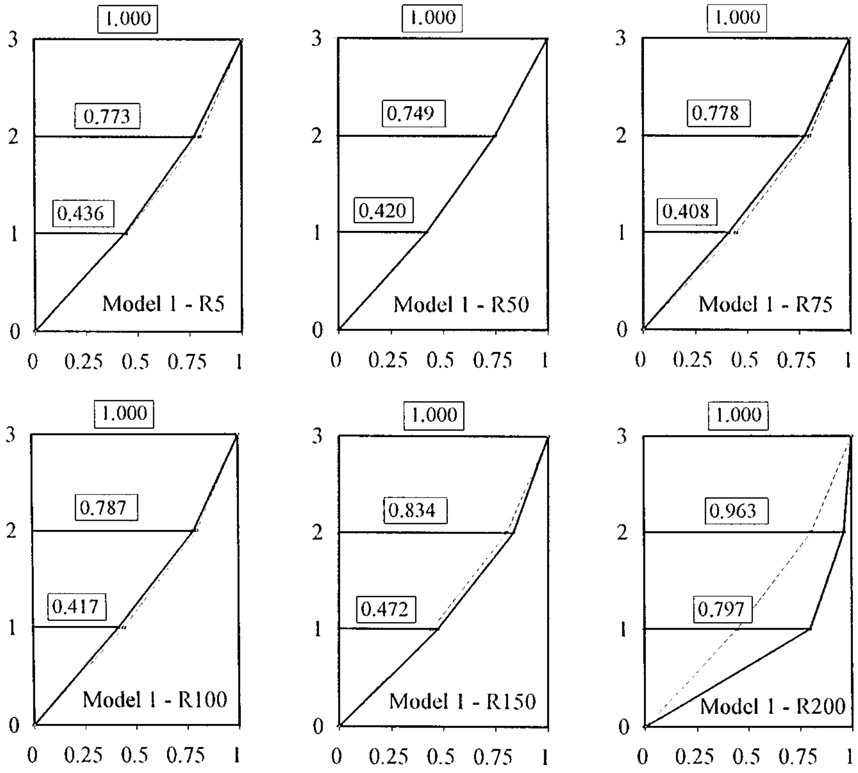

Figure 7. First natural vibration mode shapes

Table IV. First natural frequency and coefficient of equivalent viscous damping

		Model M1			Model M2		
	Test run	(1)	(2)	(3)	(1)	(2)	(3)
f (Hz)	Virgin model	22·0	21·9	—	21·4	21·9	—
	R50	21·4	20·3	15·6	15·9	15·8	15·2
	R75	17·4	17·2	14·3	13·5	12·9	10·9
	R100	15·6	14·1	11·9	8·5	8·2	8·8
	R150	7·1	6·3	7·0	4·5	4·1	3·3
ξ (%)	Virgin model	4·8	6·7	—	3·7	4·0	—
	R50	5·3	9·9	9·9	5·9	9·0	6·1
	R75	7·2	13·7	10·8	8·0	11·2	5·5
	R100	9·8	21·8	7·7	10·1	14·3	5·4
	R150	19·1	25·2	9·5	15·1	17·4	15·3

Frequency: (1) impact hammer response—after the test
(2) Fourier spectrum of impact hammer response—after the test
(3) Fourier spectrum of seismic response—during the test
Damping: (1) logarithmic decrement, impact hammer response—after the test
(2) half-power band-width, impact hammer response—after the test
(3) hysteretic damping, seismic response—during the test

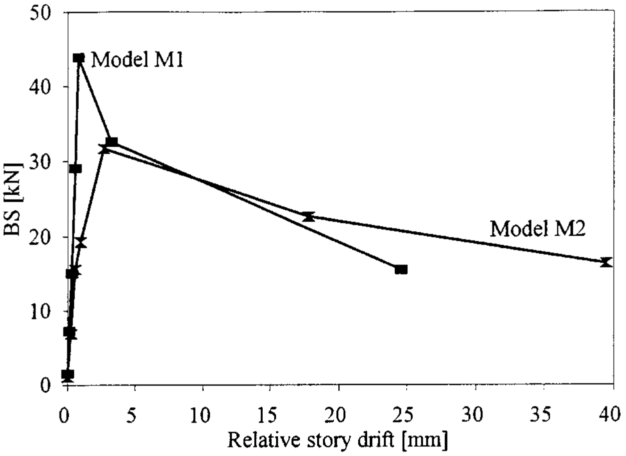

Figure 8. Base shear—first storey drift hysteresis envelopes

Table V. Stiffness degradation at characteristic limit states

Model	Storey	K_e (kN/mm)	$K_{H\max}$ (kN/mm)	$K_{H\max}/K_e$	$K_{d\max}$ (kN/mm)	$K_{d\max}/K_e$
	3	24·09	35·46	1·47	1·87	0·08
M1	2	28·62	38·75	1·35	0·49	0·02
	1	51·04	54·11	1·06	0·63	0·01
	3	15·96	9·52	0·60	8·74	0·55
M2	2	19·19	9·24	0·45	2·19	0·11
	1	27·28	11·81	0·43	0·41	0·02

The relationship between the base shear and relative storey displacement for both models is shown in Figure 8. As can be seen, because of different distribution of structural walls in longitudinal (M1) and transverse direction (M2), different strengths and rigidities have been measured. Mainly because of longitudinal central wall, not pierced with window and door openings, the rigidity of the model tested in longitudinal direction was greater than that of the model tested transversely. As regards the lateral resistance attained in longitudinal direction, the differences were not so significant. Obviously, the ultimate mechanism and contribution of vertical r.c. confining elements to the resistance of model buildings reduced the differences observed in the rigidity during the monolithic phase of behaviour.

On the basis of storey shear—relative storey drift hysteresis loops, the values of storey stiffness and hysteretic damping have been evaluated for each oscillation cycle. In the analysis, storey stiffness was defined as the average value of secant stiffness between two amplitude peaks (peak-to-peak stiffness). As can be seen in Table V, stiffness degradation is in good correlation with the observed damage to models and the measured first natural frequency decay.

Mechanism of action of tie-columns

As the analysis of the measured lateral load–strain of reinforcement relationships indicated, monolithic behaviour of the confined wall's section and alteration of strain in the tie-columns' reinforcing bars from

Table VI. Seismic resistance of prototype buildings

Direction	Limit state	Max. ground acceleration (g)	Base shear coefficient	Dynamic amplification factor
Longitudinal	Elastic limit (R75)	0·57	1·14	2·05
	Maximum resistance (R100)	0·84	1·73	2·99
	Ultimate state (R200)	1·67	0·61	0·43
Transverse	Elastic limit (R50)	0·42	0·61	2·40
	Maximum resistance (R100)	0·82	1·25	1·83
	Ultimate state (R200/1)	1·38	0·64	0·66

compression to tension has been observed at the beginning of test, at small amplitudes of vibration. After severe cracks in the masonry wall panel developed at large amplitudes of vibration, tension in reinforcing bars prevailed at both directions of vibration. This indicates that interaction forces between the masonry wall panel and r.c. tie-columns developed, inducing additional compressive stresses in the masonry panel. Once cracked, the masonry panel pushed the tie-columns sidewards and induced tension in the reinforcing bars in both directions of vibration of the model structure. The measured relationships are in good correlation with the results of tests of single confined masonry wall panels subjected to constant vertical and cyclic lateral loading.[10] On the basis of damage observation and measurements of strain induced in the tie-columns it can be concluded that the shear walls can be modelled as frames, consisting of piers represented by confined masonry walls, and spandrels represented by parapets, bond-beams and effective part of floor slabs in the direction of seismic action. Spandrels behave as coupling beams, which connect the walls and transfer bending moments.

Seismic resistance of prototype buildings

Modelling scale factors, given in Table II, should be used for referring the model test results to prototype buildings. Since the values of the base shear and story shear have been determined on the basis of the measured accelerations, the calculated values should be multiplied by acceleration scale factor $S_a = 0{\cdot}58$ when referred to as prototype values. The values of maximum ground acceleration, base shear coefficient (base shear to weight of the building ratio) and dynamic amplification factor (maximum response to shaking-table acceleration ratio) at elastic limit, maximum resistance and at ultimate state, are given in Table VI.

As can be seen, the maximum resistance of prototype buildings is relatively high. Longitudinally and transversely, the three-storey confined masonry building will be able to withstand, with limited damage to the walls, a strong earthquake with peak ground acceleration (PGA) corresponding to $0{\cdot}8g$. Energy dissipation capacity of the structure will prevent the building from collapse even in the case when subjected to subsequent stronger shaking with PGA exceeding $1{\cdot}3g$. However, at this level of earthquake ground motion, the damage caused to masonry wall panels will be beyond repair.

The analysis of seismic resistance of the tested building type indicates that, even if classified as 'simple building' according to EC 8, and without any verification of seismic resistance, the structural configuration will ensure the buildings the required degree of seismic resistance. It should be borne in mind that the required wall/floor area for simple confined masonry buildings is 5 per cent (actual values are 5·0 per cent in longitudinal and 5·6 per cent in transverse direction of the building).

SEISMIC RESISTANCE VERIFICATION

Storey resistance envelope

In case that the relationship between the resistance of the critical storey and corresponding storey drift can be assessed, the seismic resistance of the building can be verified by simple comparing the storey resistance envelope with the design seismic action and global ductility requirements. The idea to analyse the resistance of a structure by step-wise increasing the lateral loads, acting on the structure, and modifying the system when plastic hinges develop, is not new (push-over method). However, once the maximum resistance is attained and the structure is changed into a mechanism, it is no longer possible to follow the deformations by calculation. Therefore, instead of lateral loads, lateral displacements are imposed to the structure. In this way, resistance of structural elements to imposed displacements can be followed all the way up to the structure's collapse.

When this idea has been first applied to masonry buildings,[11] a simple pier mechanism action of walls has been assumed. Today, the shear walls, pierced by window and door openings, are modelled as frames, so that additional axial forces, developed in the piers due to overturning moments, are automatically taken into account. Because of structural configuration of confined masonry structures, however, these forces have little effect on the resistance. On the basis of relevant mechanism, the storey resistance envelope is evaluated as a superposition of resistance envelopes of all structural walls in the storey considered. The assumption of rigid horizontal floor diaphragm action makes possible the distribution of seismic actions among the piers according to their stiffnesses. In case that the shear wall consists of flanged sections of piers (corner walls, T, + shape sections), the contribution of the flange should be taken into account.[6] However, in the case of the verification for shear, the web, i.e. part of the wall parallel to seismic action, represents the resisting element. Because of low G/E ratio of masonry and, hence, predominant shear deformations in the case of squat walls, the assumption that the walls are separated along vertical joints is sometimes acceptable even in the case of flanged walls, where good connection between the adjoining walls is provided.

Assuming triangular distribution of displacements along the height of the building, the structure is displaced by a small value. The shear walls are deformed according to the assumed structural model and the resisting forces in structural members are calculated. Since the mass centres of individual storeys are displaced, torsional rotation might take place. In such a case, the displacements of individual piers are accordingly modified. The calculation is repeated step-by-step by increasing the imposed displacements. Once the walls enter into the non-linear range, the structural system of the building and stiffness matrices are modified. Stiffness and resistance of individual walls in each step of calculation are determined considering the calculated storey displacement and idealized resistance envelopes of structural walls in each storey.

As a result of calculation, relationship between the resistance of the critical storey and interstorey drift, i.e. the resistance envelope is obtained. At the given lateral displacement of the ith wall d_i, the resisting storey shear H_{tot} is determined as a sum of resistances of structural walls H_i in the storey considered:

$$H_{\mathrm{tot}} = \sum_i^n H_i \tag{2}$$

where the resistance of the ith wall H_i depends on the deformation of the wall d_i. In case that the resistance envelope of structural walls is idealized with trilinear relationship,[10] the following simple conditions determine the contributing stiffness and resistance of individual structural walls (Figure 9):

$$H_i = d_i K_{\mathrm{e}i};\ K_i = K_{\mathrm{e}i} \quad \text{if } d_i \leqslant d_{\mathrm{e}i}, \tag{3a}$$

$$H_i = H_{\mathrm{cr}} + \beta_1 (d_i - d_{\mathrm{e}i});\ K_i = \frac{H_i}{d_i} \quad \text{if } d_{\mathrm{e}i} < d_i \leqslant d_{\mathrm{Hmax}i}, \tag{3b}$$

$$H_i = H_{\max} - \beta_2(d_i - d_{H\max});\ K_i = \frac{H_i}{d_i} \quad \text{if } d_{\mathrm{Hmax}} < d_i \leqslant d_{\mathrm{u}i} \tag{3b}$$

$$H_i = 0;\ K_i = 0 \quad \text{if } d_i > d_{\mathrm{u}i}, \tag{3c}$$

where d_{ei}, $d_{H\max}$, d_{ui} are the displacement of the ith wall at elastic limit, maximum resistance and ultimate state, respectively, H_{cr}, $H_{\max}$ the crack limit and resistance capacity of the ith wall, respectively, β_1, β_2 the stiffness degradation parameters, K_i, K_{ei} the stiffness and effective stiffness if the ith wall, respectively, and n the number of walls.

By using relevant equations for shear and flexural resistance and stiffness of confined masonry walls, developed within a previous study,[10] the resistance envelopes corresponding to models M1 and M2 have been calculated. The calculated envelopes are correlated with the experimentally obtained curves in Figure 10. As can be seen, good correlation between experimental and calculated envelopes has been

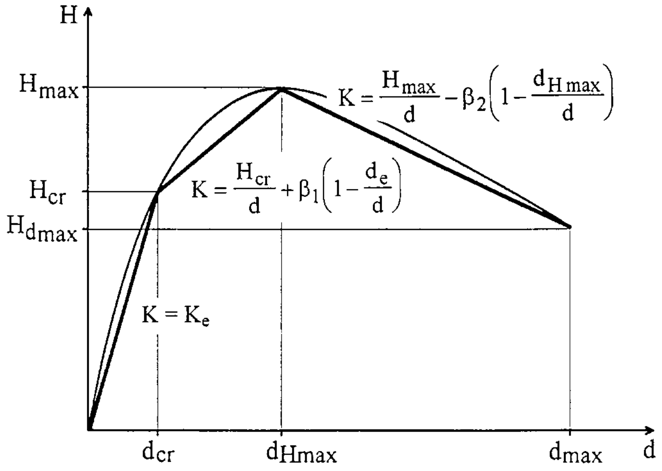

Figure 9. Idealization of experimentally obtained resistance envelope of a confined masonry wall

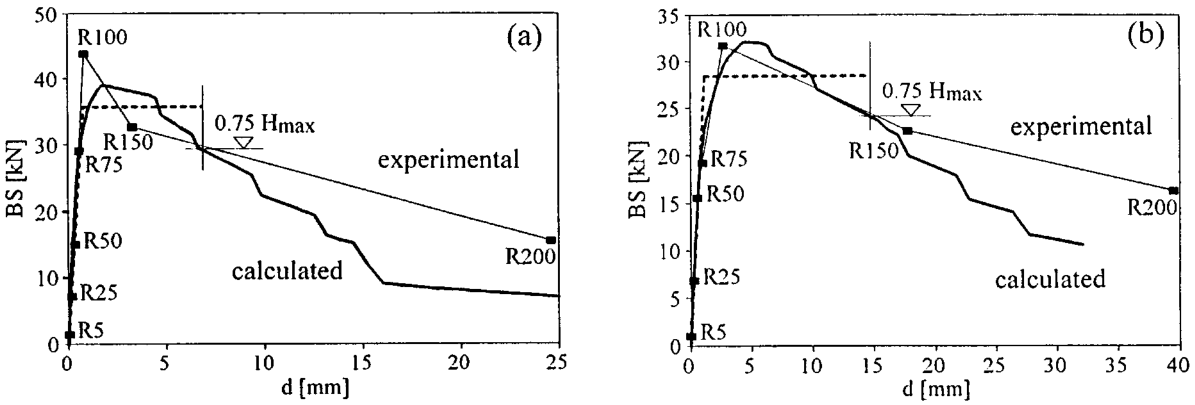

Figure 10. Comparison between experimental and calculated storey resistance envelopes. (a) Model M1 and (b) model M2

obtained in both cases, which indicates the practical validity of the proposed model for seismic resistance verification of confined masonry structures.

If, in the case of seismic resistance verification, the ultimate resistance and ductility of the structure conform with code requirements (base shear, required ductility factor), the seismic resistance of the building is adequate.

Behaviour factor

As a result of ductility and energy dissipation capacity, there is usually no need that the structure be designed for strength, i.e. for the expected elastic seismic load H_E. The structure is designed for the ultimate load H_u. The factor of reduction of elastic loads, expressed in a simplified way as a ratio between the two, is called behaviour factor, or force reduction factor $q = H_E/H_u$.

Taking advantage of the obtained experimental data, an attempt has been made to assess the value of structural behaviour factor for the case of the tested models. The actual resistance H_u of the tested prototype buildings, complying with the requirements of EC 8 for simple buildings, where seismic resistance verification is not mandatory, by far exceeded the expected design value even in severe seismic situation. Therefore, in the particular case studied, q factor has been evaluated by assuming that maximum intensity of simulated earthquake ground motion represented the design level of seismic loading. To estimate the behaviour factor according to most simple definition, the experimentally obtained base shear—relative storey displacement curve has been compared with the response of a hypothetical structure with ideal elastic characteristics to maximum shaking-table motion, which the models had resisted. As a result of this comparison, the values of behaviour factors $q = H_E/H_u = 2{\cdot}91$ and $q = 2{\cdot}47$ have been obtained for models M1 and M2, respectively, (Figure 11).

The conclusion can be therefore made that confined masonry structures possess more energy dissipation capacity than attributed to by the proposed values of behaviour factor q. However, taking into consideration the fact that limitation of story drift is necessary to avoid excessive damage to structural walls (see Figure 5), the value of q factor proposed by EC 8 seems reasonable. Similar conclusions have been obtained by an analytical study that investigated q factors for confined masonry buildings subjected to Chilean earthquakes.[11]

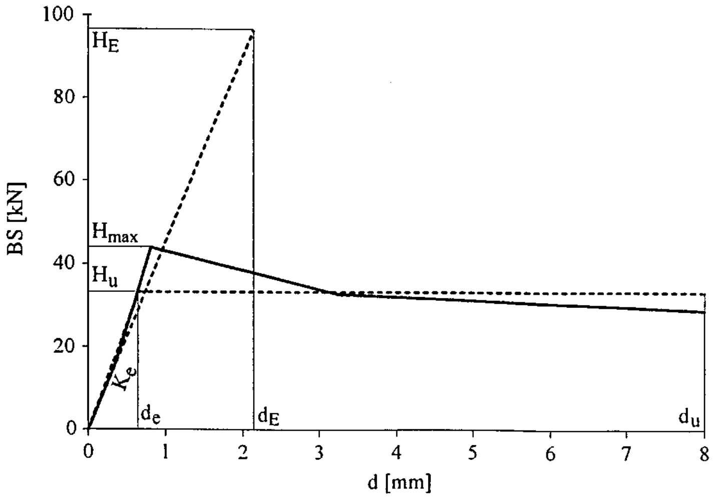

Figure 11. Evaluation of behavior factor q for the case of model M1

Within a previous experimental study,[12] the values of behaviour factors $q = 2{\cdot}84$ and $q = 3{\cdot}74$ have been obtained for unreinforced and reinforced masonry buildings of similar configuration and size, respectively. Correlating the values obtained for all three types of masonry construction, it can be seen that EC 8 values of q factors, proposed for unreinforced ($q = 1{\cdot}5$), confined ($q = 2{\cdot}0$) and reinforced masonry buildings ($q = 2{\cdot}5$), adequately reflect the assumed differences in the behaviour of different types of masonry structures, but slightly underestimate their energy dissipation capacity. However, further experimental and analytical research is needed to confirm these observations.

CONCLUSIONS

Seismic behaviour of confined masonry buildings has been experimentally investigated. Two 1:5 scale models of a typical three-storey structure, which conforms to the requirements of EC 8 for simple buildings in plan, have been tested on a shaking-table by subjecting them to a series of simulated seismic ground motions with increased intensity of shaking in each successive test run. The structural system consisted of perimetral shear walls, pierced with window and door openings, and two internal walls, which separated the plan of the building into four units. Tie-columns have been placed at all corners and wall intersections, as well as along the vertical edges of window and door openings. Wall/floor area exceeded 5 per cent in both orthogonal directions.

Predominant shear-type mechanism defined the seismic behaviour of the models. In all stories, diagonal cracks formed in the walls at the attainment of maximum resistance, whereas crushing of concrete and rupture of reinforcement of tie-columns with falling out of masonry in the first storey defined the ultimate state. With the increased damage to structure, the first natural frequency of vibration decayed, but energy dissipation increased.

The model test results indicate that prototype buildings of the tested type and size will be able to withstand, with moderate damage to the walls, strong earthquakes with peak ground acceleration of $0{\cdot}8g$, and will not collapse when subjected to repeated shaking with PGA of more than $1{\cdot}3g$. On the basis of the observed behaviour it can be concluded that the requirements of EC 8 for simple confined masonry buildings are to severe. Although the tested models represented prototypes of good-quality masonry, the actual resistance by far exceeded the expected seismic loads (design ground acceleration $a_g = 0{\cdot}3g$ in the zones of high expected seismicity).

The measured response of the models has been used to obtain data regarding the values of behaviour factor q proposed by EC 8 for confined masonry structures. Although the buildings, simple by definition of EC 8, have not been designed by calculation, the obtained values of behaviour factor q indicate that the requirements of EC 8 regarding the design seismic actions, might be relaxed. However, further experimental and analytical studies are needed to confirms these observations.

Model test results have been also used to propose a rational method for seismic resistance verification of confined masonry structures. Taking into consideration the predominant first vibration mode shape and shear-beam type shape of vibration, the storey resistance envelope is calculated by modelling the shear walls as frames. By imposing triangularly distributed of displacements along the height of the building, the structure is displaced step by step and the resistance of shear walls to imposed displacements is calculated. Good correlation between experimental and calculated envelopes has been obtained in the particular case studied, indicating the usability of the proposed method.

ACKNOWLEDGMENTS

The research discussed in this contribution has been financed by the Ministry of Science and Technology of the Republic of Slovenia (project J2-5208-1502). As regards the experimental part of the project, the contribution of the author's colleague Mr. Ljubo Petković is gratefully acknowledged.

REFERENCES

1. Eurocode 8, *Design Provisions for Earthquake Resistance of Structures. Part 1-3: General Rules—Specific Rules for Various Materials and Elements*, ENV 1998-1-3: 1995, 1995.
2. Eurocode 6, *Design of Masonry Structures. Part 1-1: General Rules for Buildings. Rules for Reinforced and Unreinforced Masonry*, ENV 1996-1-1: 1995, 1995.
3. V. Aguila, F. Delfin and M. Astroza, 'Estudio experimental de soluciones de reparacion y refuerzo para elementos de albanileria'. *Pub. SES I 1/88* (221), Universidad de Chile, Santiago, 1988.
4. Y. Wenzhong and J. Zhaohong, 'Functions of ties concrete columns in brick walls' *Proc. 9th World Conf. Earthquake Engng*., Tokyo-Kyoto **6**, 139–144 (1988).
5. G. Aguilar, R. Meli, R. Diaz and R. Vasquez-del-Mercado, 'Influence of horizontal reinforcement on the behavior of confined masonry walls', *Proc. 11th World Conf. Earthquake Engng*., Acapulco, paper no.1380 (1996).
6. M. Iiba, H. Mizuno, T. Goto and H. Kato, 'Shaking table test on seismic performance of confined masonry wall', *Proc. 11th World Conf. Earthquake Engng*., Acapulco, paper no. 659, 1996.
7. Z. Bolong, W. Mingshun and Z. Deyuan, 'Shaking table study of a five-story unreinforced block masonry model building strengthened with reinforced concrete columns and tie bars', *Proc*., *US-PRC Joint Workshop on Seismic Resistance of Masonry Struct*., Harbin, IV-11; 1-11, 1988.
8. *Bulletin of the Strong-Motion Earthquake Accelerograms. No. 1*, *IZIIS*, Skopje, 1984.
9. A. Arias, 'A measure of earthquake intensity', in *Seismic Design of Nuclear Power Plants* (R. Hanson, ed.), MIT Press, Cambridge, MA, 1970.
10. M. Tomaževič and I. Klemenc, L. Petković and M. Lutman, 'Seismic behaviour of confined masonry buildings. Part two: shaking-table tests of model buildings M1 and M2—analysis of test results'. *Report ZAG/PI-95/06*, Ljubljana (1996).
11. M. O. Moroni, M. Astroza and J. Gomez, 'Seismic force reduction factors for masonry buildings', *Proc. 10th World Conf. Earthquake Engng*., 8, Madrid, 1992, pp. 4521–4524.
12. M. Tomaževič and P. Weiss, 'Seismic behavior of plain- and reinforced-masonry buildings', *J. Struct. Engng*. (ASCE) **120**, 323–338 (1994).